

This is an Open Access document downloaded from ORCA, Cardiff University's institutional repository:<https://orca.cardiff.ac.uk/id/eprint/109254/>

This is the author's version of a work that was submitted to / accepted for publication.

Citation for final published version:

West, Ryan A., Cunningham, Thomas, Pennicott, Lewis E., Rao, Srinivasa P. S. and Ward, Simon 2018. Toward more drug like inhibitors of trypanosome alternative oxidase. *ACS Infectious Diseases* 4 (4) , pp. 592-604. 10.1021/acsinfecdis.7b00218

Publishers page: <http://dx.doi.org/10.1021/acsinfecdis.7b00218>

Please note:

Changes made as a result of publishing processes such as copy-editing, formatting and page numbers may not be reflected in this version. For the definitive version of this publication, please refer to the published source. You are advised to consult the publisher's version if you wish to cite this paper.

This version is being made available in accordance with publisher policies. See <http://orca.cf.ac.uk/policies.html> for usage policies. Copyright and moral rights for publications made available in ORCA are retained by the copyright holders.



Towards more drug like inhibitors of trypanosome alternative oxidase

Ryan A. West ^a, Thomas Cunningham ^a, Lewis E. Pennicott ^a, Srinivasa P. S. Rao ^b, Simon E. Ward*
^{a, c}

^a Sussex Drug Discovery Centre, University of Sussex, Brighton, BN1 9QJ, United Kingdom.

^b Novartis Institutes for Tropical Diseases, 5300 Chiron Way, California, 94608-2916, USA.

^c Medicines Discovery Institute, Park Place, Cardiff University, CF10 3AT, United Kingdom, Wards10@cardiff.ac.uk.

New tools are required to ensure the adequate control of the neglected tropical disease human African trypanosomiasis. Annual reports of infection have recently fallen to fewer than 5000 cases per year; however, current therapies are hard to administer and have safety concerns, hence are far from ideal. Trypanosome alternative oxidase is an exciting target for controlling the infection; it is unique to the parasite and inhibition of this enzyme with the natural product ascofuranone has shown to clear *in vivo* infections. We report the synthesis and associated structure activity relationships of inhibitors based upon this natural product with correlation to *T. b. brucei* growth inhibition in an attempt to generate molecules that possess improved physicochemical properties and potential for use as new treatments for human African trypanosomiasis.

Keywords: Medicinal chemistry, drug design, multiparameter optimisation, human African trypanosomiasis.

Human African trypanosomiasis (HAT), otherwise known as African sleeping sickness, is a neglected tropical disease caused by human infection by the protozoan parasites *T. b. gambiense* or *T. b. rhodesiense*, transmitted by tsetse flies in sub-Saharan Africa.¹ Without treatment, HAT is invariably fatal;² the drugs that are currently approved for treatment of both the haemolymphatic (stage 1) and encephalitic (stage 2) phases of the disease have either toxic side effects or require complex administration procedures.³ Resistant strains of the parasites have been observed in the clinic and there is a requirement for new treatment options to guarantee the successful control of the disease.^{4,5} In 2009 it was estimated that occurrences of the disease had fallen below 20 000 incidences a year and that 65 million people are at risk of transmission.¹

The trypanosome, first discovered by Sir David Bruce in 1894,⁶ undergoes diverse lifecycle adaptations conferring viability in both the tsetse fly vector and mammalian host.^{7,8} A predominant feature of *Trypanosoma brucei* is that it is capable of successfully evading host immune responses, predominantly due to its capacity to diversify the surface antigens that it presents to its host;⁹ this ability has been a major factor for preventing the development of an efficacious vaccine against the pathogen.¹⁰ *T. b. gambiense* is responsible for >95% of cases of HAT and is a zoonotic disease, residing in a variety of domestic animals and livestock.¹¹ Trypanosome infection in cattle and other livestock also has a large burden on the health and associated economic output of animals; the cost of delivering trypano-

cidal agents to control 'Nagana' or African animal trypanosomiasis (AAT) is estimated to be 140 million USD per year.¹²

Current treatments for HAT are far from ideal. Stage 1 of the disease is treated with suramin for *T. b. rhodesiense* or pentamidine for *T. b. gambiense*, both compounds display undesired toxic side effects in the clinic.¹³ Resistance against pentamidine has also been observed and linked to mutations in the P2 amino purine and other trypanosome uptake transporters.⁵ Both suramin and pentamidine are unable to permeate into the CNS to sufficient levels, and thus are ineffective against stage 2 infections.¹⁴ The organo-arsenide melarsoprol and the more recent combination therapy of nifurtimox and eflornithine (NECT) are currently used to treat infections of *T. b. gambiense* and *T. b. rhodesiense* respectively. Both treatments have their limitations. Melarsoprol shows significant toxic effects in those treated, causing encephalopathy in 5-10% of people treated with the drug.¹⁵ Incidences of resistance to melarsoprol are becoming more commonplace, again linked to mutations in the P2 amino purine uptake transporters; associated failure rates in the clinic have been reported to be between 20%-30% in the early 2000's.⁵ NECT requires the administration of eflornithine *via* slow intravenous infusion of 200 mg/kg every 12 hours for 7 days as it is only trypanostatic, thus requiring trypanocidal action by the co-administered nifurtimox and innate host clearance mechanisms.¹⁶

With the limitations of the currently approved medicines for treating HAT and the increasing reports of resistance to these therapies, it is vital to discover new and improved treatments against the pathogen. An ideal target for drug discovery for HAT is the trypanosome alternative oxidase (TAO).¹⁷ TAO is the sole terminal oxidase enzyme in the

aerobic respiratory pathway for the long slender blood stage form of *Trypanosoma brucei* subspecies. The enzyme utilises oxygen and ubiquinol as substrates for the efficient generation of cellular ATP as the parasite does not express regular cytochrome respiratory complexes.¹⁸ TAO is a di-iron (non-heme) oxidoreductase that is located in the inner-mitochondrial membrane of the trypanosome.¹⁹ As TAO is not found in mammalian systems, there is a unique opportunity to attain compounds with enhanced selectivity and circumvent on-target toxicity.¹⁹ It has recently been reported that the pentamidine and melarsoprol drug resistant parasites have an increased sensitivity to inhibition of TAO, as these parasites have a reduced capacity to efflux cellular glycerol that is produced as the result of anaerobic respiration.²⁰ The crystal structure of TAO has been reported, allowing a structure based design approach to new molecules.²¹ Nanomolar inhibition of TAO has been reported with the natural product ascofuranone (AF (**1**)) and its analogues in validated biochemical assays,²² demonstrating correlation in *ex vivo* growth inhibition²³ and efficacy in *in vivo* clearance models.²⁴

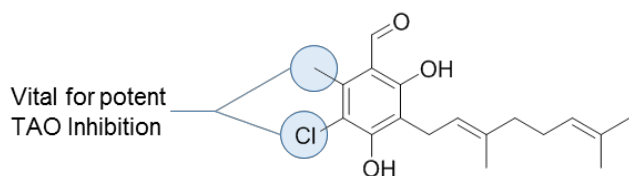


Figure 1. Summary of previous work²³

Our previous work identified robust synthetic routes to close analogues of AF (**1**) and structure activity relationships of the synthesized molecules, highlighting the requirement of both the chloro and methyl substituents on the aromatic ring for high potency (figure 1).²³ With these routes in place we set out to further explore structurally similar analogues with the aim to reduce lipophilicity, and improve the drug like properties of these molecules. Our aim of reducing lipophilicity was to specifically improve aqueous solubility, decrease metabolism and improve the potential to achieve efficacious CNS concentrations, as new compounds for HAT must be effective against both stages of the disease.

There are many hurdles preventing permeability of organic drug molecules to the brain. The blood brain barrier provides significant protection to xenobiotics; tight junctions around capillaries prevent permeation and the expression of ABC-transporters actively transport solubilised organic molecules out and away from the barrier and the brain.²⁵ Compounds that traverse readily into the CNS tend to have high passive permeability, have low efflux from ABC-transporters like P-glyco-protein (P-gp) and have low metabolic turnover in human liver microsomes, providing the basis for the generation of a predictive scoring tool for CNS penetration.²⁶

A major contribution to the poor multi-parameter optimisation (MPO)²⁶ predicted CNS-penetration score for AF (**1**) and colletochlorin B (CCB (**2**)) is attributed to its high lipophilicity. Clearly the major contributor to the high lipophilicity of CCB (**2**) is from the geranyl 'lipophilic tail' (figure 2). Compounds with a cLogP above 5 are commonly observed to be P-gp substrates, and tend to have a high metabolic liability. We herein report the synthesis and SAR investigation of analogues focused on reducing the lipophilicity of the tail region of structural analogues of AF (**1**) and CCB (**2**), with an aim to improve physicochemical properties and increase the predicted CNS penetration MPO score.

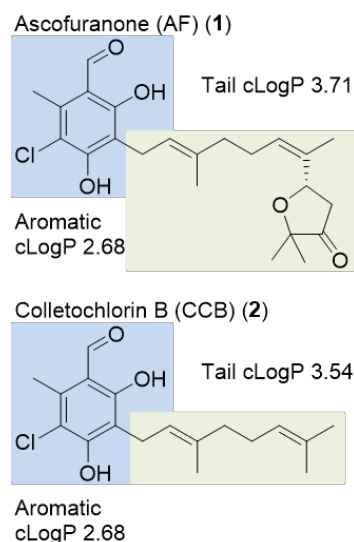


Figure 2. Per atom contribution to lipophilicity of ascofuranone (AF) (**1**) and colletochlorin B (CCB) (**2**)

Results and Discussion

The biochemical assessment of the bicyclic 1,2-isoxazole intermediate prepared to access the aldehyde replacement with the nitrile analogue of CCB (**2**), had shown unexpectedly high potency for inhibiting TAO. Previous reports had postulated that a hydrogen bond donor was needed at this position for potent inhibition of TAO.²²

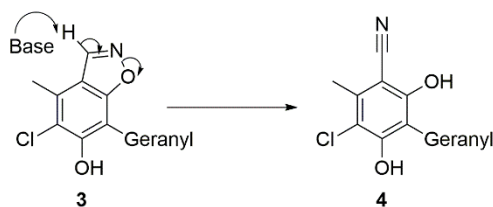
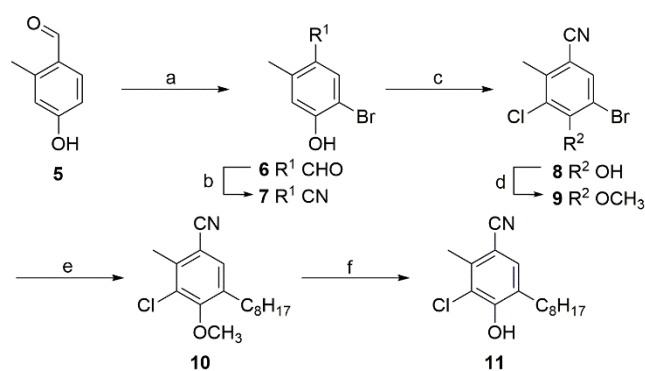


Figure 3. Isoxazole Kemp elimination

To confirm this result, a synthetic route to the mono phenolic compound (**11**) was devised (scheme 1), to rule out the activity arising from an *in situ* formation of nitrile compound *via* a Kemp elimination (figure 3).²⁷

Scheme 1. Mono-phenol analogue synthesis



Reaction conditions: a) trimethylphenylammonium tribromide, CH₂Cl₂ / MeOH rt, 3 h, 77%, b) NH₂OH·HCl, EtOH, reflux, 16 h, 90%, c) NCS, Et₃N, MeCN, 0°C – rt, 16 h, 70%, d) dimethyl sulfate, acetone, rt, 16 h, 98%, e) i) BH₃·THF, 1-octene, 0°C, 20 min, ii) toluene, H₂O, K₃PO₄, RuPhos, Pd(OAc)₂, 50°C, 16 h, 90% f) TMS-Cl, NaI, MeCN, 80°C, 16 h, 65%.

Selective bromination of the phenolic aldehyde was achieved by treatment with trimethylbenzylammonium tribromide at 0 °C; non-selective and over bromination was observed using *N*-bromosuccinimide.²⁸ The aldehyde (6) could be successfully converted to the nitrile (7) by oxime formation with hydroxylamine hydrochloride and subsequent *in situ* dehydration. Protection of the phenol (8) to the anisole (9) with dimethylsulfate was required to facilitate a high yielding Suzuki-Miyaura cross-coupling using tri-*n*-octylborane as the coupling partner that was formed *in situ* by reacting 1-octene with a solution of 1M borane in THF.²⁹ Final deprotection of the anisole (10) to the free phenol using trimethylsilyl chloride and sodium iodide provided the monophenol analogue (11) for biochemical and *ex vivo* assessment (table 1).³⁰

Table 1. Biological assay assessment of isoxazole and mono-phenol analogues

#	Structure	TAO pIC ₅₀ [†]	<i>T. b. b.</i> pEC ₅₀ [*]	HepG2 pCC ₅₀ [#]
2		8.5 ± 0.3	8.4 ± 0.1	5.1 ± 0.1
4		8.4 ± 0.2	6.4 ± 0.1	4.9 ± 0.1
3		8.3 ± 0.4	7.0 ± 0.2	5.3 ± 0.2
11		8.9 ± 0.3	7.6 ± 0.1	5.1 ± 0.1
46		7.0 ± 0.1	5.1 ± 0.2	4.7 ± 0.1
10		4.5 ± 0.1	< 4.3	< 4.3

[†]: Negative log concentration and standard deviation of compounds required for 50% inhibition of trypanosome alternative oxidase; ^{*}: Negative log concentration and standard deviation of compounds required for 50% growth inhibition of *T. b. brucei* Lister427; [#]: Negative log concentration and standard deviation of compounds required for 50% cytotoxicity of HepG2 cell line. (n ≥ 2 in all assays)

Interestingly, the monophenol analogue (11) retained high potency against TAO that corresponded to the most potent

inhibition of *T. b. brucei* growth for a compound not containing the benzaldehyde functionality present in AF and

CCB. The removal of one of the flanking substituents *ortho* to the brominated coupling position facilitated its reactivity and thus exploration of this tail. This synthetic route was adopted for further diversification of this tail region. The des-methyl starting material was accessible from commercially available sources and was used to initially investigate tail modifications.

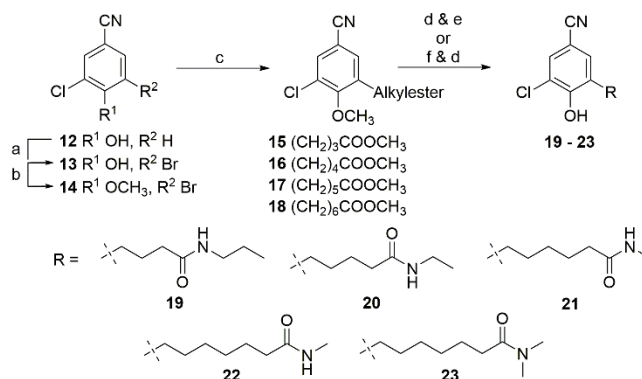
The introduction of polarity into the lipophilic tail was devised to reduce cLogP and improve upon the predicted CNS penetration MPO score (>4 required for high predicted CNS exposure). The introduction of amide functionality in alternate positions in the chain were planned to mimic the *n*-octyl (C₈H₁₇) or geranyl chain. The inclusion of the amide functionality had the largest predicted improvement to both cLogP and MPO score (Row C – table 2). 1-Alkene esters were converted to trialkylboranes using the methodology previously employed to access the *n*-octyl analogues (scheme 2). These were then coupled with the brominated intermediate (**14**). The esters were converted to the desired amides by either *in situ* hydrolysis under the demethylation conditions, with subsequent HATU amide coupling with the required alkylamine, or a direct aminolysis of the ester by using 1,5,7-triazabicyclo[4.4.0]dec-5-ene (TBD) and the desired alkylamine with subsequent anisole deprotection with TMSCl / NaI to provide the amide chain compounds for biological assessment (table 3).³¹

Table 2. cLogP and predicted MPO scores for planned analogues.

Row	Structure	cLogP	MPO Score ²⁶
A (4)		6.2	3.5
B (11)		6.3	3.8
C		3.5	5.5
D		4.6	4.8
E (43)		4.9	4.2

cLogP calculated from ChemAxon Marvin Sketch, calculated MPO as described by Wager *et al.*²⁶

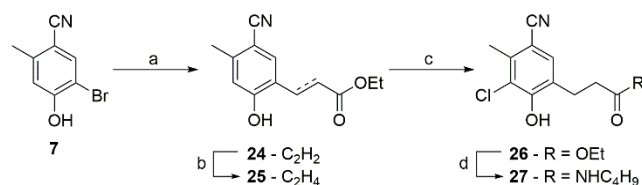
Scheme 2. Amide tail linker synthesis



Reaction conditions: a) NBS, MeCN, rt, 16 h, 85%, b) dimethyl sulfate, acetone, reflux, 3 h, 90%, c) i) BH₃·THF, 1-alkene ester, 0 °C, 20 min, ii) toluene, H₂O, K₃PO₄, RuPhos, Pd(OAc)₂, 16 h, 50 °C, 90%, d) TMSCl, NaI, MeCN, 80 °C, 16 h, 35-85%. e) HATU, Et₃N, R¹R²NH, MeCN, rt, 3 h, 60-90%, f) TBD, R¹R²NH, MeCN, rt, 1 – 16 h 70-85%.

The acrylic ester could not be successfully coupled under these conditions; we postulate that the required trialkylborane may not form as the alkene is too electron deficient. The desired ester was synthesized by a Heck-Mizoroki cross-coupling and subsequent reduction of the double bond, before chlorination and amide formation with TBD (scheme 3).

Scheme 3. Heck cross-coupled amide tail linker synthesis

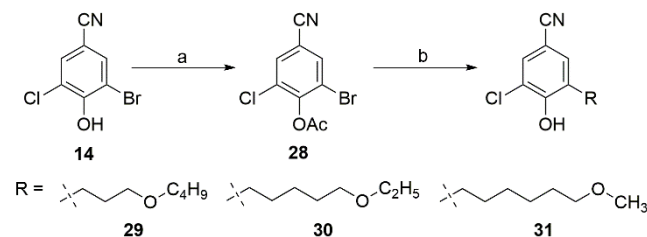


Reaction conditions: a) ethyl acrylate, SingaCycle™, K₂CO₃, NMP, 100 °C, 16 h, 30%, b) triethylsilane, Pd/C, EtOH, rt, 16 h, 78%, c) SO₂Cl₂, Et₂O, rt, 96 h, 57%, d) TBD, *n*-butylamine, MeCN, 16h, 39%.

A selection of ether chain analogues were also planned and synthesised (**D** – table 2), these were expected to be more chemically similar to that of the aliphatic chain with a smaller amount of polarity introduced in comparison to the amide. These compounds were less chemically tractable; in our hands the anisole de-protection to the phenol proved challenging. The deprotection conditions that we explored led to the cleavage of the desired ether functionality present in the chain to the terminal alcohol. To mitigate this synthetic hurdle, alternative protecting groups were investigated. Bulkier silyl protecting groups hindered the cross-coupling and failed to provide the desired ether tail analogues. Reaction with the phenolic ester (**27**) provided some cross-coupled product, the stability of this protecting group perhaps unsurprisingly, proved to be labile under the reaction coupling conditions. The de-acetylated products (**29** to **31**) were observed and isolated from the reactions however significant proportions of the starting material ester (**28**) saponified before cross-coupling providing

a major by-product of the deacetylated phenol (**14**) thus resulting in lower isolated yields (scheme 4).

Scheme 4. Ether tail linker synthesis



Reaction conditions: a) Ac_2O , pyridine, DCM, rt, 16 h, 74%, b) i) $\text{BH}_3\cdot\text{THF}$, 1-alkene ether, 0°C , 20 min, ii) toluene, H_2O , K_3PO_4 , RuPhos, $\text{Pd}(\text{OAc})_2$, 16 h, 50°C , 7-24%.

Table 3. Biological assessment of polar tail analogues

#	R^3	R^5	cLogP	TAO pIC_{50}^\dagger	<i>T. b. brucei</i> pEC_{50}^*
11		CH_3	6.3	8.9 ± 0.3	7.6 ± 0.1
46		H	5.8	7.0 ± 0.1	5.1 ± 0.2
27		CH_3	3.5	5.5 ± 0.2	<4.3
19		H	3.0	<4.5	-
20		H	2.9	4.6 ± 0.1	-
21		H	3.0	4.6 ± 0.1	-
22		H	3.4	5.1 ± 0.1	<4.3
23		H	3.6	5.4 ± 0.2	<4.3
29		H	4.1	4.8 ± 0.1	4.7 ± 0.1
30		H	4.1	5.6 ± 0.1	4.6 ± 0.1
31		H	4.1	5.2 ± 0.1	<4.3

† : Negative log concentration and standard deviation of compounds required for 50% inhibition of trypanosome alternative oxidase; * : Negative log concentration and standard deviation of compounds required for 50% growth inhibition of *T. b. brucei* Lister427. ($n \geq 2$ in all assays performed).

This data suggested that a lipophilic tail was required for the potent inhibition of TAO. To further probe this observation; analogues were prepared to assess the length of tail needed for potent inhibition of TAO and whether total lipophilicity could be decreased by reduction of the carbon chain length (E – table 2). Previous reports had shown large

Assessment of these less lipophilic analogues showed a large decrease in potency compared to the *n*-octyl analogues, highlighting that even minor increases in polarity in this part of the lipophilic tail was not tolerated. The most promising analogues included polarity at the terminal of the chain (**22** and **23**); however, disappointingly, these compounds resulted in no measurable inhibition of *T. b. brucei* growth (table 3).

decreases in potency against TAO at carbon chain length below 3. The C1-7 analogues (**39** to **45**) were prepared in a similar fashion to that of the *n*-octyl analogue (**11**); C1-4 analogues were however prepared directly using the alkyl boronic acid or trimeric alkyl boroxines as the volatile alkene hydrocarbons were not accessible (scheme 5).

Scheme 5. Carbon chain length analogue synthesis

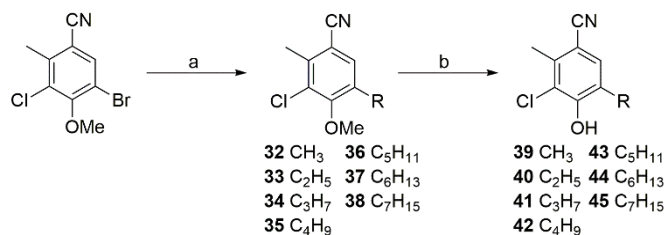
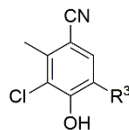


Table 4. Biological assessment of carbon chain length analogues



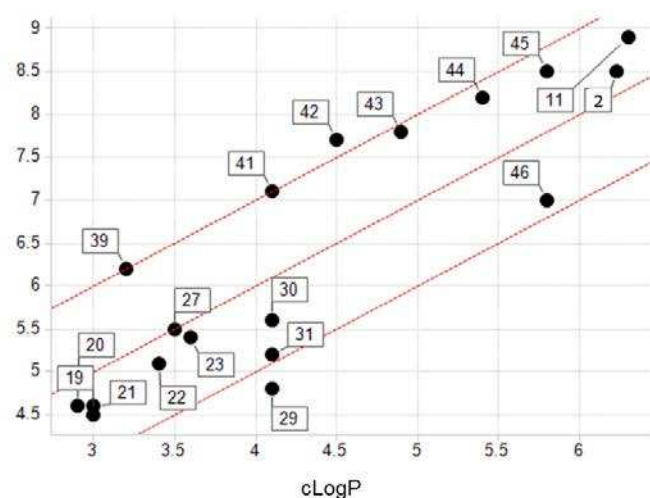
#	R ³	cLogP	TAO pIC ₅₀ [†]	T. b. b. pEC ₅₀ [*]
11	<i>n</i> -C ₈ H ₁₇	6.3	8.9 ± 0.3	7.6 ± 0.1
45	<i>n</i> -C ₇ H ₁₅	5.8	8.5 ± 0.1	6.6 ± 0.2
44	<i>n</i> -C ₆ H ₁₃	5.4	8.2 ± 0.1	6.1 ± 0.1
43	<i>n</i> -C ₅ H ₁₁	4.9	7.8 ± 0.1	6.0 ± 0.1
42	<i>n</i> -C ₄ H ₉	4.5	7.7 ± 0.1	5.3 ± 0.1
41	<i>n</i> -C ₃ H ₇	4.1	7.1 ± 0.1	4.7 ± 0.1
39	<i>n</i> -CH ₃	3.2	6.2 ± 0.1	4.7 ± 0.1

[†]: Negative log concentration and standard deviation of compounds required for 50% inhibition of trypanosome alternative oxidase; ^{*}: Negative log concentration and standard deviation of compounds required for 50% growth inhibition of *T. b. brucei* Lister427. ($n \geq 2$ for all assays performed).

Interestingly, the reduced carbon chain length analogues showed good potency against TAO (table 4), until a notable decrease in enzymatic inhibition was observed at compounds with C₃ or below, corroborating previous reports.²² What was more evident was the decrease observed in efficacy against *T. b. brucei* growth inhibition as chain length

and cLogP decreased. Compounds showed a distinct drop off in potency against *T. b. brucei* for each carbon reduction. To interrogate this data further correlations of cLogP and biochemical and cellular potency were carried out (figure 4).

TAO pIC₅₀



T. b. b. pEC₅₀

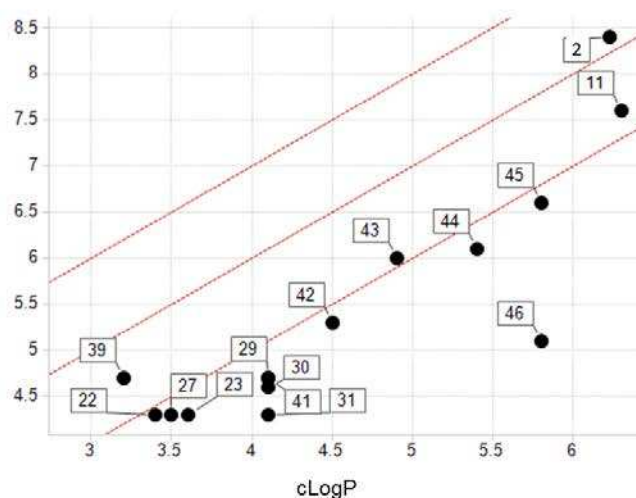


Figure 4. Correlations of cLogP vs TAO inhibition pIC₅₀ (left) and cLogP vs *T. b. b.* pIC₅₀ growth inhibition (right). LipE is lipophilic ligand efficiency (pIC₅₀ – cLogP)³².

Biochemical potency for these compounds track to a lipophilic ligand efficiency of 3. Cellular potency, however correlates to a lipophilic ligand efficiency of 1, relating to a 100-fold decrease in potency from the biochemical activity to the cellular assay. The 2 log decrease in cellular potency observed here could be due a combination of reasons that we are currently investigating, it is of interest that CCB (2) shows a smaller decrease in potency from the biochemical to cellular assay. The permeability of the compounds though the cell and mitochondrial membranes of the trypanosome may reduce as the lipophilicity decreases. The compounds could be substrates for efflux transport, that may reduce the intracellular concentration. The TAO inhibition kinetics of the compounds may be altered with the reduction in carbon chain length that could result in faster dissociation, resulting in reduced efficacy on target. The compounds may not locate to the desired cell compartment as lipophilicity may be required for the inhibitors to be retained in the inner mitochondrial membrane where the enzyme is located. Colletochlorin B could be acting on an unknown complimentary anti-parasitic target. On-going studies to better understand these data will aid future analogue design and synthesis to identify more drug like inhibitors of TAO.

We also noticed positive correlation between cLogP and both biochemical and cellular activity (figure 4). Examples of potency correlating to high lipophilicity have previously been observed with other membrane proteins and enzymes requiring lipophilic substrates.^{33,34}

Conclusions

HAT continues to provide a challenge for the development of new therapies; cases continue to be reported with resistance more frequently observed. Discoveries of new brain penetrant *T. b. gambiense* and *T. b. rhodesiense* trypanocides are vital for ensuring the adequate control of HAT in the future. Our work in this area has been to identify potent inhibitors of TAO that possess improved physicochemical properties than that of the natural products from which they are derived. Our exploration in this area has previously shown the requirement for the methyl and chloro substituents on the aromatic ring for high potency inhibition of TAO. Our efforts reported here for modulating the lipophilicity of this molecule by the introduction of polar functionality in the tail region of this chemotype has proved challenging. Polar functionality in this region of the molecule was shown to not be tolerated with large decreases in potency against TAO observed. The reduction in the carbon chain length of the tail resulted in identifying analogues that retained high inhibitory activity of TAO, however *ex vivo* efficacy against *T. b. brucei* growth was diminished. We will continue to try to understand this disconnect and use this generated data for future compound design towards more drug like inhibitors of TAO.

Materials and Methods

Experimental Details. ChemAxon Calculator Plugins were used for structure property prediction and calculation (cLogP), Marvin 15.5.4, 2015, ChemAxon (<http://www.chemaxon.com>). All commercial reagents were purchased from Sigma-Aldrich, Alfa Aesar, Apollo Scientific, Fluo-rochem or Tokyo Chemical Industry and of the highest available purity. Unless otherwise stated, chemicals were used as supplied without further purification. Anhydrous solvents were purchased from Acros (AcroSeal™) or Sigma-Aldrich (SureSeal™) and were stored under nitrogen. 40-60 petrol ether refers to the fraction with a boiling point between 40 °C and 60 °C. Anhydrous solvents and reagents were used as purchased. Thin layer chromatography (TLC) was carried out using glass plates pre-coated with Merck silica gel 60 F254. Melting points were determined using an OptiMelt apparatus and are uncorrected. Proton nuclear magnetic resonance spectra were recorded at 500 MHz on a Varian VNMR5 500 MHz spectrometer (at 30 °C), using residual isotopic solvent (CHCl₃, δ = 7.27 ppm, DMSO δ = 2.50 ppm, MeOH δ = 3.31 ppm) as an internal reference. Chemical shifts are quoted in parts per million (ppm). Coupling constants (J) are recorded in Hertz (Hz). Carbon nuclear magnetic resonance spectra were recorded at 125 MHz on a Varian 500 MHz spectrometer and are proton decoupled, using residual isotopic solvent (CHCl₃, δ = 77.00 ppm, DMSO δ = 39.52 ppm, MeOH δ = 49.00 ppm) as an internal reference. Proton and carbon spectra assignments are supported by DEPT editing. High resolution mass spectrometry (HRMS) data (ESI) was recorded on Bruker Daltonics, Apex III, ESI source: Apollo ESI with methanol as spray solvent. Only molecular ions, fractions from molecular ions and other major peaks are reported as mass/charge (m/z) ratios. LCMS data was recorded on a Waters 2695 HPLC using a Waters 2487 UV detector and a Thermo LCQ ESI-MS. Samples were eluted through a Phenomenex Lunar 3 µm C18 50 mm × 4.6 mm column, using water and acetonitrile acidified by 0.1% formic acid at 1 ml/min and detected at 254 nm. The gradient employed was a 7 min method 30-90% MeCN over a 5 min gradient, held at 90% MeCN for 1 min, then re-equilibrated to 30% MeCN over 1 min. All experiments were carried out under an inert atmosphere of N₂ unless otherwise stated.

TAO Absorbance Assay. 1-Ubiquinol turnover was measured by recording the increase in absorbance at 278 nm (Greiner 96-well UV star flat bottom plates with BMG PHERAstar FS photo spectrometer) to monitor the increase of 1-ubiquinone concentration kinetically over 6 min with purified rTAO (3 nM). A final concentration of 15 µM 1-ubiquinol was used under the following conditions: 50 mM Tris-HCl; 0.05% (w/v) C10E8; pH 7.4; 25 °C). The sigmoidal curve of the inhibition was observed by 10-point 3-fold serial dilution of test compounds to generate IC₅₀ values.

Growth inhibition assays. Bloodstream form *Trypanosoma brucei brucei* Lister 427 parasites were continuously

passed in HMI-9 medium formulated from IMDM medium (Invitrogen), 10% heat-inactivated fetal bovine serum, 10% Serum Plus medium supplement (SAFC Biosciences), 1 mM hypoxanthine (Sigma-Aldrich), 50 μ M bathocuproine disulfonic acid (Sigma-Aldrich), 1.5 mM cysteine (Sigma-Aldrich), 1 mM pyruvic acid (Sigma-Aldrich), 39 μ g / mL thymidine (Sigma-Aldrich), and 14 μ L / L beta-mercapthoethanol (Sigma-Aldrich); all concentrations of added components refer to that in complete HMI-9 medium. The parasites were cultured in 10 mL of HMI-9 medium in T75 CELL-STAR tissue culture flasks at 37 °C / 5% CO₂.

To determine growth inhibitory potency of compounds against *T. b. brucei* bloodstream form parasites, 200 nL of 10-point, 3-fold serially diluted compounds in DMSO were transferred to the wells of white, solid bottom 384-well plates (Greiner Bio-One) by either Echo 555 acoustic liquid handling system or Mosquito. Then, 104 of *T. b. brucei* parasites in 40 μ L of HMI-9 medium were added to each well, and the plates were incubated for 48 hours at 37 °C in 5% CO₂ incubators. Parasite numbers in individual plate wells were determined through quantification of intracellular ATP amount. The CellTiter-Glo luminescent cell viability reagent (Promega) was added to plate wells, and ATP-dependent luminescence signal was measured on Tecan M1000 plate Reader after 30 min incubation. Suramin an anti-trypanosomal drug was used positive control and DMSO was used as negative control. pIC₅₀ values were calculated using Graph Pad Prism software by plotting the luminescence values in sigmoidal dose response curves. Suramin was used as a positive control in screening. (pIC₅₀ 6.7 \pm 0.1)

Hep-G2 Cytotoxicity Assay. Human hepatocellular carcinoma (HepG2) cells were obtained from ATCC and grown in RPMI media. 25 μ L of 1.6 x 10⁴ cells / mL were dispensed into sterile 384 well Griener clear plates and incubated at 37 °C in 5% CO₂ incubator for 24 h. Once the cells adhered, 125 nL of 10-point, 3-fold serially diluted compounds in DMSO were transferred on to cells. After incubating for additional 96 h at 37 °C in 5% CO₂ incubator, cells were added with CCK-8 reagent to each well. Plates were further incubated for 3 h followed by absorbance reading at 450 nM using Envision reader. Absorbance values were used for determination of cytotoxic concentration (pCC₅₀) required to inhibit 50% growth. Purmycin was used as positive control in screening (pCC₅₀ 6.3 \pm 0.1).

Synthesis

5-Chloro-7-[(2E)-3,7-dimethylocta-2,6-dien-1-yl]-1,2-benzoxazol-6-ol (3)

To a solution of triphenylphosphine (42 mg, 0.16 mmol) in dichloromethane (2 mL) was added 2,3-dichloro-5,6-dicyano-*p*-benzoquinone (37 mg, 0.16 mmol). The dark reaction mixture was stirred at room temperature for 1 minute during which time the colour faded. 4-Chloro-2-(2E)-3,7-dimethylocta-2,6-dien-1-yl]-6-[(hydroxyimino)m ethyl]benzene-1,3-diol (35 mg, 0.10 mmol) in dichloromethane (0.5 mL) was added to the reaction mixture in 1 portion and this was stirred for 1 minute before being concentrated under

reduced pressure. Purification by flash column chromatography (10 g silica), eluting with a gradient of petrol ether : ethyl acetate (100 : 0) to (90 : 10), gave the title compound as a white solid (24 mg, 72%). ¹H NMR (500 MHz, Chloroform-d) δ 8.60 (s, 1H), 6.10 (s, 1H), 5.42 – 5.32 (m, 1H), 5.10 – 5.01 (m, 1H), 3.66 (d, J = 7.3 Hz, 2H), 2.58 (s, 3H), 2.11 – 2.05 (m, 2H), 2.05 – 1.98 (m, 2H), 1.84 (d, J = 1.2 Hz, 3H), 1.64 (d, J = 1.4 Hz, 3H), 1.57 (d, J = 1.2 Hz, 3H).

2-Methyl-4-hydroxy-5-bromo-benzaldehyde (6)

To a solution of 2-methyl-4-hydroxy-benzaldehyde (10 g, 73.45 mmol) in CH₂Cl₂ (100 mL) and methanol (50 mL) was added a solution of phenyltrimethylammonium tribromide (30.07 g, 77.12 mmol) in CH₂Cl₂ : methanol (1:1, 100 mL) at -5 °C. The reaction was warmed to ambient temperature and stirred for 16 h. The reaction was concentrated under reduced pressure and the residue was added 1 M HCl (aq) (200 mL) to precipitate a white solid, the solid was collected by filtration and dried under reduced pressure to give the title compound as a cream precipitate (14.67 g, 94 %): m.p. 160–165 °C, (methanol / water). IR (neat, ν_{\max}) cm⁻¹, 3063, 1384, 1310, 1136. ¹H NMR (500MHz, D₆-DMSO) δ 11.35 (1H, br s), 9.95 (1H, s), 7.91 (1H, s), 6.83 (1H, s), 2.49 (3H, s). ¹³C NMR (126MHz, D₆-DMSO) δ 190.8 (CH), 159.2 (C), 142.3 (C), 137.1 (CH), 128.0 (C), 119.1 (CH), 107.4 (C), 19.1 (CH₃). HRMS (ESI⁻) *m/z* [M-H]⁻ calculated for C₈H₆BrO₂ 212.9557, found 212.9550.

5-Bromo-4-hydroxy-2-methyl-benzonitrile (7)

A solution of 2-methyl-4-hydroxy-5-bromo-benzaldehyde (20.00 g, 93.0 mmol), in acetonitrile (300 mL) was added hydroxylamine hydrochloride (6.92 g, 99.5 mmol). The reaction mixture was heated to reflux and stirred for 16 hours. The reaction mixture was cooled to 50 °C and added further hydroxylamine hydrochloride (1.5 g, 21.5 mmol). The reaction mixture was heated to reflux for a further 3 hours. This was collected by filtration and dried under vacuum to give 13.08 g of an off-white solid. Analysis showed a good purity product. The filtrate was concentrated under vacuum. The residue was triturated in MeCN : water (1:2) and sonicated, the solid was collected by filtration and dried under vacuum, to provide a further 6.67 g (19.75, quant.). m.p. 194-199 °C (MeCN / water). IR (neat, ν_{\max}) cm⁻¹ 3203, 2232 (CN), 1595, 1402, 1386, 1260, 1221. ¹H NMR (500MHz, D₆-DMSO) - δ 11.38 (1H, br s), 7.90 (1H, s), 6.92 (1H, s), 2.49 (3H, s). ¹³C NMR (126MHz, D₆-DMSO) δ 158.6 (C), 143.4 (C), 137.1 (CH), 117.9 (CH), 117.7 (C), 107.3 (C), 103.8 (C), 19.1 (CH₃). HRMS (ESI⁻) *m/z* [M-H]⁻ calculated for C₈H₅BrNO 209.9560, found 209.9554.

5-Bromo-3-chloro-4-hydroxy-2-methyl-benzonitrile (8)

Triethylamine (0.83 mL, 5.97 mmol) was added to a solution of 5-bromo-2-methyl-4-hydroxybenzonitrile (1.15 g, 5.42 mmol) in acetonitrile (50 mL). 1-chloropyrrolidine-2,5-dione (1.52 g, 11.38 mmol) was added portionwise to the stirring solution. To the reaction mixture was added water (50 mL), precipitating a pale-yellow solid that was collected by filtration to provide the title compound (1.11 g, 83%). m.p. 166-169 °C, IR (neat, ν_{\max}), cm⁻¹ 3239, 2236 (CN), 1581, 1468, 1384, 1294, 1224, 1147. ¹H NMR (500MHz, CDCl₃) δ 7.70 (s, 1H), 6.39 (s, 1H), 2.58 (s, 3H). ¹³C NMR (126 MHz,

CDCl₃) δ 152.5 (C), 140.9 (C), 134.4 (CH), 122.1 (CH), 116.4 (C), 107.5 (CH), 106.9 (C), 19.0 (CH₃). HRMS (ESI⁻) m/z [M-H]⁻ calcd for C₈H₄BrClNO 243.9170, found 243.9165.

5-Bromo-3-chloro-4-methoxy-2-methyl-benzonitrile (**9**)

Dimethyl sulfate (0.85 mL, 8.95 mmol) was added to a suspension of 5-bromo-3-chloro-4-hydroxy-benzonitrile (2.10 g, 8.52 mmol), and potassium carbonate (1.41 g, 10.22 mmol) in acetone (80 mL). The reaction mixture was heated to reflux for 3 hours, the reaction was cooled to RT and added water (160 mL) precipitating a white solid that was collected by vacuum filtration to give the title compound (2.07 g, 93%). m.p. 119-120 °C, IR (neat, ν_{\max}), cm⁻¹ 2229 (CN), 1457, 1372, 1275, 1048. ¹H NMR (500 MHz, CDCl₃) δ 7.74 (s, 1H), 3.94 (s, 3H), 2.58 (s, 3H). ¹³C NMR (126 MHz, CDCl₃) δ 157.4 (C), 141.7 (C), 134.9 (CH), 131.3 (C), 116.3 (C), 116.0 (C), 111.0 (C), 61.0 (CH₃), 19.2 (CH₃). LRMS EI⁺ 261 m/z .

3-Bromo-5-chloro-4-hydroxybenzonitrile (**13**)

N-Bromosuccinimide (0.30 g, 1.71 mmol) was added to a solution of 3-chloro-4-hydroxybenzonitrile (0.25g, 1.63 mmol) in acetonitrile (5 mL). To the reaction mixture was added water (15 mL), precipitating a white solid, this was collected by filtration and dried under reduced pressure to provide the title compound as a white solid (0.36 g, 84%). m.p. 166-169 °C. IR (neat, ν_{\max}), cm⁻¹ 3411, 2229, 1471, 1327, 1294, 1245, 1204, 1156. ¹H NMR (500MHz, CDCl₃) δ 7.75 (s, 1H), 7.64 (s, 1H) 6.37 (s, 1H). ¹³C NMR (126 MHz, CDCl₃) δ 152.8 (C), 135.0 (C), 132.6 (CH), 121.7 (C), 116.3 (C), 110.9 (C), 106.1 (C). HRMS (ESI⁻) m/z [M-H]⁻ calcd for C₇H₂BrClNO 229.9014, found 231.8984.

3-Bromo-5-chloro-4-methoxybenzonitrile (**14**)

Dimethyl sulfate (0.15 mL, 1.61 mmol) was added to a suspension of potassium carbonate (0.22 g, 1.61 mmol) and 3-bromo-5-chloro-4-hydroxy-benzonitrile (0.30 g, 1.29 mmol) in acetone (10 mL). The reaction mixture was heated to reflux for 30 min, cooled to RT and added water. The resulting precipitate was collected by filtration and dried under reduced pressure to provide the title compound as a white solid (0.29 g, 90%). m.p. 115-116 °C, IR (neat, ν_{\max}), cm⁻¹ 2236 (CN), 1539, 1470, 1419, 1272. ¹H NMR (500MHz, CDCl₃) δ 7.78 (s, 1H), 7.66 (s, 1H), 3.97 (s, 3H). ¹³C NMR (126 MHz, CDCl₃) δ 157.6 (C), 135.4 (CH), 133.2 (CH), 130.4 (C), 119.5 (C), 116.0 (C), 109.9 (C), 61.0 (CH₃). HRMS (ESI⁻) m/z [M-H]⁻ calcd for C₈H₅BrClNO 243.9170, found 243.9165.

(2-Bromo-6-chloro-4-cyano-phenyl) acetate (**28**)

3-Bromo-5-chloro-4-hydroxy-benzonitrile (500 mg, 2.15 mmol) was dissolved in dichloromethane (10 mL), before pyridine (0.26 mL, 3.23 mmol) and acetic anhydride (0.24 mL, 2.58 mmol) were added. The reaction mixture was stirred at room temperature for 12 h. The reaction mixture was taken up in water (10 mL) and the organic components were washed with water (2 × 10 mL). The chlorinated layer was separated, washed with brine (1 × 10 mL), dried over MgSO₄, filtered and concentrated in vacuo, to give the title compound as a granular white solid (462 mg, 74%). m.p. 116-119 °C; IR (neat, ν_{\max} , cm⁻¹) 3088, 2238, 1774; ¹H NMR (500 MHz, CDCl₃) δ 7.83 (s, 1H), 7.72 (s, 1H), 2.44 (s, 3H);

¹³C (126 MHz, CDCl₃) δ 166.3 (C), 149.3 (C), 135.0 (CH), 132.7 (CH), 130.3 (C), 119.3 (C), 115.7 (C), 112.2 (C), 20.3 (CH₃); LRMS m/z (EI⁺) 275.

General protocol for alkene cross-couplings

1-Alkene (2.54 mmol) was dropwise added to an ice cooled solution of 1M borane in THF (0.91 mmol). This solution was warmed to room temperature and stirred for 15 min. The solution was quenched with the addition of water (0.25 mL), and diluted with toluene (2.5 mL). Potassium phosphate tribasic (0.43 g, 2.03 mmol), aromatic bromide (1.01 mmol), palladium(II) acetate (0.01 g, 0.025) mmol and 2-dicyclohexylphosphino-2'-6'-diisopropoxybiphenyl (0.02 g, 0.05 mmol) were added. The reaction mixture sealed and heated 100°C for 16 hours. The reaction mixture was partitioned between water (10 mL) and EtOAc (20 mL). The organic layer was separated, dried over MgSO₄, filtered and concentrated under vacuum. The residue was purified by flash silica chromatography, eluting with petroleum ether to 10-50% EtOAc followed by purification by preparative HPLC 50% MeCN in water to 100% MeCN to provide the title compounds (11-90%).

3-Chloro-4-methoxy-2-methyl-5-octyl-benzonitrile (**10**)

IR (neat, ν_{\max}) cm⁻¹ 2913, 2849, 2226 (CN), 1468, 1291, 1074. ¹H NMR (500 MHz, CDCl₃) δ 7.36 (s, 1H), 3.87 (s, 3H), 2.62 (t, *J* = 7.9 Hz, 2H), 2.57 (s, 3H), 1.61-1.55 (m, 2H), 1.36-1.27 (m, 10H), 0.89 (t, *J* = 6.8 Hz, 3H). ¹³C NMR (126 MHz, CDCl₃) δ 158.2 (C), 139.4 (C), 136.3 (C), 132.0 (CH), 129.7 (C), 117.7 (C), 109.4 (C), 60.9 (CH₃), 31.8 (CH₂), 30.2 (CH₂), 29.7 (CH₂), 29.4 (CH₂), 29.3 (CH₂), 29.1 (CH₂), 22.6 (CH₂), 18.8 (CH₃), 14.0 (CH₃). LRMS EI⁺ 293 m/z .

5-Chloro-4-methoxy-5-octylbenzonitrile (**46** intermediate)

IR (neat, ν_{\max}) cm⁻¹ 2925, 2854, 2232 (CN), 1470, 1426, 1275. ¹H NMR (500 MHz, CDCl₃) δ 7.53 (s, 1H), 7.40 (s, 1H), 3.90 (s, 3H), 2.66 (t, *J* = 7.9 Hz, 2H), 1.60 (m, 2H), 1.40 – 1.26 (m, 10H), 0.90 (t, *J* = 6.8 Hz, 3H). ¹³C NMR (126 MHz, CDCl₃) δ 158.2 (C), 139.7 (C), 132.4 (CH), 131.7 (CH), 128.9 (C), 117.7 (C), 108.5 (C), 61.1 (CH₃), 31.8 (CH₂), 30.2 (CH₂), 29.4 (CH₂), 29.3 (CH₂), 29.1 (CH₂), 22.6 (CH₂), 14.0 (CH₃). HRMS (ESI⁻) m/z [M-H]⁻ calcd for C₁₅H₁₉ClNO 264.1161, found 264.1153.

Methyl 4-(3-chloro-5-cyano-2-methoxy-phenyl)butanoate (**15**)

IR (neat, ν_{\max}), cm⁻¹ 2952, 2231 (CN), 1732, 1427, 1276, 993, 877. ¹H NMR (500 MHz, CDCl₃) δ 7.55 (d, *J* = 2.1 Hz, 1H), 7.40 (d, *J* = 2.1 Hz, 1H), 3.90 (s, 3H), 3.68 (s, 3H), 2.70 (t, *J* = 7.7 Hz, 2H), 2.36 (t, *J* = 7.3 Hz, 2H), 1.92 (m, 2H). ¹³C NMR (126 MHz, CDCl₃) δ 158.2 (C), 139.7 (C), 132.4 (CH), 131.7 (CH), 128.9 (C), 117.7 (C), 108.5 (C), 61.1 (CH₃), 31.8 (CH₂), 30.2 (CH₂), 30.0 (CH₂), 29.4 (CH₂), 29.3 (CH₂), 29.1 (CH₂), 22.6 (CH₂), 14.0 (CH₃). LRMS EI⁺ 267 m/z .

Methyl 5-(3-chloro-5-cyano-2-methoxy-phenyl)pentanoate (**16**)

IR (neat, ν_{\max}), cm⁻¹ 2951, 2233 (CN), 1733, 1472, 1275. ¹H NMR (500 MHz, CDCl₃) δ 7.53 (s, 1H), 7.38 (s, 1H), 3.89 (s, 3H), 3.67 (s, 3H), 2.67 (m, 2H), 2.35 (m, 2H), 1.65 (m, 4H). ¹³C NMR (126 MHz, CDCl₃) δ 173.8 (C), 158.2 (C), 139.9 (C),

132.4 (C), 132.0 (C), 128.9 (C), 117.6 (C), 108.5 (C), 61.1 (CH₃), 51.6 (CH₃), 33.7 (CH₂), 29.7 (CH₂), 29.5 (CH₂), 24.6 (CH₂). LRMS EI+ 281 m/z.

Methyl 6-(3-chloro-5-cyano-2-methoxy-phenyl)hexanoate (17)

IR (neat, ν_{\max} , cm⁻¹) 2948, 2232 (CN), 1733, 1472, 1275. ¹H NMR (500 MHz, CDCl₃) δ 7.53 (s, 1H), 7.38 (s, 1H), 3.89 (s, 3H), 3.67 (s, 3H), 2.65 (m, 2H), 2.32 (m, 2H), 1.70-1.57 (m, 4H), 1.39 (m, 2H). ¹³C NMR (126 MHz, CDCl₃) δ 174.0 (C), 158.2 (C), 139.2 (C), 132.4 (CH), 131.9 (CH), 128.9 (C), 117.7 (C), 108.5 (C), 61.1 (CH₃), 51.5 (CH₃), 33.8 (CH₂), 29.82 (CH₂), 29.80 (CH₂), 28.8 (CH₂), 24.6 (CH₂). LRMS EI+ 295 m/z.

Methyl 7-(3-chloro-5-cyano-2-methoxy-phenyl)heptanoate (18)

IR (neat, ν_{\max} , cm⁻¹) 2933, 2232 (CN), 1734, 1472, 1276. ¹H NMR (500 MHz, CDCl₃) δ 7.52 (s, 1H), 7.38 (s, 1H), 3.88 (s, 3H), 3.66 (s, 3H), 2.64 (m, 2H), 2.31 (m, 2H), 1.66-1.55 (m, 4H), 1.36 (m, 4H). ¹³C NMR (126 MHz, CDCl₃) δ 174.3 (C), 158.4 (C), 139.6 (C), 132.6 (CH), 132.0 (CH), 129.1 (C), 117.9 (C), 108.6 (C), 61.3 (CH₃), 51.7 (CH₃), 34.1 (CH₂), 30.14 (CH₂), 30.08 (CH₂), 29.2 (CH₂), 29.0 (CH₂), 24.9 (CH₂). HRMS (ESI⁺) m/z [M+Na]⁺ calcd for C₁₆H₂₀ClNNaO₃ 332.1024, found 332.1019.

3-(3-Butoxypropyl)-5-chloro-4-hydroxy-benzonitrile (29)

IR (neat, ν_{\max} , cm⁻¹) 2923, 2236. ¹H NMR (500 MHz, CDCl₃) δ 7.51 (s, 1H), 7.31 (s, 1H), 3.50 (t, J = 6.6 Hz, 2H), 3.43 (t, J = 5.9 Hz, 2H), 2.76 (t, J = 6.9 Hz, 2H), 1.90 (p, J = 6.4 Hz, 2H), 1.62 (p, J = 7.1 Hz, 2H), 1.40 (h, J = 7.5 Hz, 2H), 0.95 (t, J = 7.5 Hz, 3H); ¹³C NMR (126 MHz, CDCl₃) δ 154.9 (C), 133.0 (CH), 131.5 (CH), 130.4 (C), 121.8 (C), 118.2 (C), 104.0 (C), 71.1 (CH₂), 68.5 (CH₂), 31.5 (CH₂), 29.0 (CH₂), 26.4 (CH₂), 19.3 (CH₂), 13.9 (CH₃); HRMS (ESI⁻) m/z [M-H]⁻ calcd for C₁₄H₁₇ClNO₂ 266.0953, found 266.0953.

3-Chloro-5-(5-ethoxypentyl)-4-hydroxy-benzonitrile (30)

¹H (500 MHz, CDCl₃) δ 7.49 (s, 1H), 7.33 (s, 1H), 3.47 (q, J = 7.1 Hz, 2H), 3.41 (t, J = 6.3 Hz, 2H), 2.66 (t, J = 7.8 Hz, 2H), 1.62 (p, J = 8 Hz, 4H), 1.40 (p, J = 7.8 Hz, 2H), 1.20 (t, J = 7.0 Hz, 3H). ¹³C (126 MHz, CDCl₃) δ 153.6 (C), 132.6 (CH), 130.4 (CH), 120.5 (C), 118.1 (C), 104.1 (C), 88.2 (C), 70.5 (CH₂), 66.2 (CH₂), 30.2 (CH₂), 29.4 (CH₂), 28.7 (CH₂), 26.0 (CH₂), 15.1 (CH₃); HRMS (ESI⁻) m/z [M-H]⁻ calcd for C₁₄H₁₇ClNO₂ 266.0953, found 266.0942.

3-Chloro-4-hydroxy-5-(6-methoxyhexyl)benzonitrile (31)

IR (neat, ν_{\max} , cm⁻¹); 2932, 2860, 2233 (CN), 1174, 1116; ¹H NMR (500 MHz, CDCl₃) δ 7.49 (s, 1H), 7.33 (s, 1H), 3.55 (s, 3H) 3.36 (t, J = 6.6 Hz, 2H), 2.65 (t, J = 7.8 Hz, 2H), 1.57 (p, J = 7.4 Hz, 4H), 1.37 (m, 4H); ¹³C (126 MHz, CDCl₃) δ 153.3 (C), 132.7 (CH), 130.3 (CH), 120.4 (C), 110.0 (C), 100.2 (C), 88.3 (C), 72.8 (C), 58.6 (C), 30.1 (CH₂), 29.5 (CH₂), 29.1 (CH₂), 28.9 (CH₂), 25.9 (CH₃); HRMS (ESI⁻) m/z [M-H]⁻ calcd for C₁₄H₁₇ClNO₂ 266.0953, found 266.0941.

3-Chloro-4-methoxy-2-methyl-5-pentyl-benzonitrile (36)

¹H NMR - (500MHz, CDCl₃) δ 7.35 (s, 1H), 3.85 (s, 3H), 2.60 (t, J = 7.8 Hz, 2H), 2.55 (s, 3H), 1.57 (t, J = 7.5 Hz, 2H), 1.41-1.18 (m, 4H), 0.89 (t, J = 6.7 Hz, 3H). ¹³C NMR - (126 MHz, CDCl₃) δ 158.1 (C), 139.4 (C), 136.3 (C), 132.0 (CH), 129.6 (C),

117.8 (C), 109.3 (C), 60.9 (CH₃), 31.5 (CH₂), 29.9 (CH₂), 29.7 (CH₂), 22.4 (CH₂), 18.8 (CH₃), 13.9 (CH₃).

3-Chloro-5-hexyl-4-methoxy-2-methyl-benzonitrile (37)

¹H NMR - (500MHz, CDCl₃) δ 7.35 (s, 1H), 3.85 (s, 3H), 2.60 (t, J = 7.6 Hz, 2H), 2.54 (s, 3H), 1.61-1.48 (m, 2H), 1.41-1.17 (m, 6H), 0.87 (t, J = 6.8 Hz, 3H). ¹³C NMR - (126 MHz, CDCl₃) δ 158.1 (C), 139.3 (C), 136.3 (C), 132.0 (CH), 129.6 (C), 117.7 (C), 109.3 (C), 60.9 (CH₃), 31.6 (CH₂), 30.1 (CH₂), 29.7 (CH₂), 29.1 (CH₂), 22.5 (CH₂), 18.8 (CH₃), 14.0 (CH₃).

3-Chloro-5-heptyl-4-methoxy-2-methyl-benzonitrile (38)

¹H NMR - (500MHz, CDCl₃) δ 7.35 (s, 1H), 3.85 (s, 3H), 2.60 (t, J = 7.9 Hz, 2H), 2.54 (s, 3H), 1.61-1.50 (m, 2H), 1.38-1.11 (m, 8H), 0.87 (t, J = 6.7 Hz, 3H). ¹³C NMR - (126 MHz, CDCl₃) δ 158.1 (C), 139.3 (C), 136.3 (C), 132.0 (CH), 129.6 (C), 117.7 (C), 109.3 (C), 60.9 (CH₃), 31.7 (CH₂), 30.8 (CH₂), 29.7 (CH₂), 29.3 (CH₂), 29.0 (CH₂), 22.6 (CH₂), 18.8 (CH₃), 14.1 (CH₃).

General protocol for alkylboronic acid Suzuki-Miyaura cross-coupling.

Dicyclohexyl-[2-(2,6-diisopropoxyphenyl)phenyl]phosphane (9 mg, 0.02 mmol) and palladium(II) acetate (2 mg, 0.01 mmol) was added to a degassed suspension of 5-bromo-3-chloro-4-methoxy-2-methyl-benzonitrile (100 mg, 0.38 mmol), boronic acid or trialkylboroxine (0.58 mmol) and tripotassium phosphate (244 mg, 1.15 mmol) in toluene (2 mL). The reaction mixture was sealed, degassed, put under a nitrogen atmosphere and heated to 100°C for 16-72 h. The reaction mixture was filtered through a pad of celite, the filtrate was partitioned between ethylacetate and water, the organics were separated, washed with brine, dried over MgSO₄, filtered and concentrated under vacuum. The residue was purified by flash chromatography eluting with petroleum ether to 10%-25% ethylacetate in petroleum ether. Material was further purified by reverse phase flash chromatography, eluting with water to MeOH if required to provide the cross-coupled analogues described (36-67%).

3-Chloro-4-methoxy-2,5-dimethyl-benzonitrile (32)

¹H NMR - (500MHz, CDCl₃) δ 7.35 (s, 1H), 3.84 (s, 3H), 2.55 (s, 3H), 2.29 (s, 3H). ¹³C NMR - (126 MHz, CDCl₃) δ 158.3 (C), 139.5 (C), 132.9 (CH), 131.5 (C), 129.6 (C), 117.6 (C), 109.2 (C), 60.2 (CH₃), 18.8 (CH₃), 16.0 (CH₃).

3-Chloro-5-ethyl-4-methoxy-2-methyl-benzonitrile (33)

¹H NMR - (500MHz, CDCl₃) δ 7.37 (s, 1H), 3.86 (s, 3H), 2.75-2.60 (m, 2H), 2.56 (s, 3H), 1.22 (t, J = 7.5 Hz, 3H). ¹³C NMR - (126 MHz, CDCl₃) δ 158.0 (C), 139.4 (C), 137.5 (C), 131.4 (CH), 129.6 (C), 117.8 (C), 109.5 (C), 60.9 (CH₃), 22.3 (CH₂), 18.8 (CH₃), 14.4 (CH₃).

3-Chloro-4-methoxy-2-methyl-5-propyl-benzonitrile (34)

¹H NMR - (500MHz, CDCl₃) δ 7.35 (s, 1H), 3.86 (s, 3H), 2.60 (t, J = 6.7 Hz, 2H), 2.55 (s, 3H), 1.66-1.56 (m, 2H), 0.96 (t, J = 7.4 Hz, 3H). ¹³C NMR - (126 MHz, CDCl₃) δ 158.2 (C), 139.4 (C), 136.0 (C), 132.1 (CH), 129.7 (C), 117.8 (C), 109.3 (C), 60.9 (CH₃), 31.7 (CH₂), 23.3 (CH₂), 18.9 (CH₃), 13.9 (CH₃).

5-Butyl-3-chloro-4-methoxy-2-methyl-benzonitrile (35)

¹H NMR - (500MHz, CDCl₃) δ 7.35 (s, 1H), 3.86 (s, 3H), 2.62 (t, J = 7.7 Hz, 2H), 2.55 (s, 3H), 1.59-1.51 (m, 2H), 1.41-1.31 (m,

2H), 0.93 (t, 3H). ^{13}C NMR - (126 MHz, CDCl_3) δ 158.1 (C), 139.4 (C), 136.3 (C), 132.1 (CH), 129.7 (C), 117.8 (C), 109.3 (C), 60.9 (CH_3), 32.3 (CH_2), 31.7 (CH_2), 22.5 (CH_2), 18.8 (CH_3), 13.8 (CH_3).

General protocol for demethylation with trimethylsilyl iodide.

Chloro(trimethyl)silane (0.26 mL, 2.0 mmol) was added to a suspension of sodium iodide (0.31 g, 2.0 mmol) and anisole (0.51 mmol) in acetonitrile (2 mL). The reaction mixture was heated to reflux for 4-96 hours. The cooled reaction mixture was partitioned between 0.1 M sodium thiosulfate (10 mL) and ethyl acetate (2 x 20 mL). The organic layers were separated, combined dried over MgSO_4 , filtered and concentrated under vacuum. The residue was purified by flash silica chromatography, eluting with petroleum ether to 30% ethyl acetate to provide the phenolic compounds (28-80%).

3-Chloro-4-hydroxy-2-methyl-5-octyl-benzonitrile (**11**)

IR (neat, ν_{max}) cm^{-1} 3360, 2928, 2850, 2222 (CN), 1601, 1473, 1461, 1163. ^1H NMR (500 MHz, CDCl_3) δ 7.31 (s, 1H), 6.08 (s, 1H), 2.64 (t, J = 7.7 Hz, 2H), 2.56 (s, 3H), 1.59 (m, 2H), 1.45-1.20 (m, 10H) 0.91 (t, J = 7.2 Hz, 3H). ^{13}C NMR (126 MHz, CDCl_3) δ 153.0 (C), 138.2 (C), 132.2 (CH), 128.9 (C), 121.0 (C), 118.0 (C), 110.0 (C), 31.8 (CH_2), 29.9 (CH_2), 29.3 (CH_2), 29.3 (CH_2), 29.2 (CH_2), 29.1 (CH_2), 22.6 (CH_2), 18.7 (CH_2), 14.0 (CH_3). HRMS (ESI^-) m/z [M-H] $^-$ calculated for $\text{C}_{16}\text{H}_{21}\text{ClNO}$ 278.1317, found 278.1303.

4-(3-Chloro-5-cyano-2-hydroxy-phenyl)butanoic acid (**19 a**)

IR (neat, ν_{max}) cm^{-1} 3345, 2569, 2228 (CN), 1691, 1474, 1253. ^1H NMR (500 MHz, CDCl_3) δ 12.06 (br s, 1H), 10.43 (br s, 1H), 7.81 (d, J = 2.0 Hz, 1H), 7.51 (d, J = 2.0 Hz, 1H), 2.61 (t, J = 7.5 Hz, 2H), 2.19 (t, J = 7.5 Hz, 2H), 1.73 (quintet, J = 7.5 Hz, 2H). ^{13}C NMR (126 MHz, CDCl_3) δ 174.6 (C), 155.6 (C), 133.1 (CH), 132.4 (C), 131.9 (CH), 121.6 (C), 118.7 (C), 102.8 (C), 33.6 (CH_2), 29.5 (CH_2), 24.5 (CH_2). HRMS (ESI^-) m/z [M-H] $^-$ calcd for $\text{C}_{11}\text{H}_9\text{ClNO}_3$ 238.0276, found 238.0266.

5-(3-Chloro-5-cyano-2-hydroxy-phenyl)pentanoic acid (**20 a**)

IR (neat, ν_{max}) cm^{-1} 3093, 2867, 2243 (CN), 1723, 1471, 1105. ^1H NMR (500 MHz, CDCl_3) δ 11.98 (br s, 1H), 10.40 (br s, 1H), 7.78 (d, J = 2.0 Hz, 1H), 7.53 (d, J = 2.0 Hz, 1H), 2.59 (t, J = 7.2 Hz, 2H), 2.20 (m, 2H), 1.49 (m, 4H). ^{13}C NMR (126 MHz, CDCl_3) δ 174.8 (C), 155.6 (C), 133.8 (C), 133.0 (C), 131.8 (C), 121.5 (C), 118.8 (C), 102.7 (C), 33.9 (CH_2), 29.8 (CH_2), 28.7 (CH_2), 24.5 (CH_2). HRMS (ESI^-) m/z [M-H] $^-$ calcd for $\text{C}_{12}\text{H}_{11}\text{ClNO}_3$ 252.0433, found 252.0423.

6-(3-chloro-5-cyano-2-hydroxy-phenyl)-N-methyl-hexanamide (**21 b**)

IR (neat, ν_{max}) cm^{-1} 3395, 2941, 2226 (CN), 1638, 1559, 1291, 1271. ^1H NMR (500 MHz, $\text{D}_6\text{-DMSO}$) δ 10.37 (br s, 1H, OH-7), 7.76 (s, 1H, CH-6), 7.67 (br s, 1H, NH-17), 7.51 (s, 1H, CH-4), 2.56 (t, J = 7.14 Hz, 2H, CH_2 -11), 2.52 (m, 3H, CH_3 -19), 2.01 (t, J = 7.2 Hz, CH_2 -15), 1.47 (m, 4H, CH_2 -12/14), 1.22 (m, 2H, CH_2 -13). ^{13}C NMR (126 MHz, $\text{D}_6\text{-DMSO}$) δ 172.9 (C16), 155.6 (C2), 133.2 (C3), 133.0 (CH-4), 131.7 (CH-6), 121.5 (C1), 118.8 (C9), 102.6 (C5), 35.6 (CH_2 -15), 29.9 (CH_2 -11), 29.0

(CH_2 -12), 28.8 (CH_2 -13), 25.8 (CH_3 -19), 25.5 (CH_2 -14). HRMS-ESI m/z [M+H] $^+$ calcd for $\text{C}_{14}\text{H}_{17}\text{ClN}_2\text{NaO}_2$ 303.0871, found 303.0865.

7-(3-Chloro-5-cyano-2-hydroxy-phenyl)-N-methyl-heptanamide (**22 b**)

^1H NMR - (500MHz, CDCl_3) δ 7.57 (d, J = 2.0 Hz, 1H), 7.40 (d, J = 2.0 Hz, 1H), 2.69 (s, 3H), 2.66 (t, J = 7.4 Hz, 2H), 2.16 (t, J = 7.6 Hz, 2H), 1.70-1.50 (m, 4H), 1.44-1.22 (m, 4H). ^{13}C NMR - (126 MHz, CDCl_3) δ 172.4 (C), 155.2 (C), 132.9 (C), 132.1 (CH), 130.8 (CH), 121.0 (C), 117.8 (C), 102.8 (C). LRMS, (ESI^+) [M+H] $^+$ 295.1 m/z .

7-(3-Chloro-5-cyano-2-hydroxy-phenyl)-N,N-dimethyl-heptanamide (**23 b**)

^1H NMR - (500MHz, CDCl_3) δ 7.48 (s, 1H) 7.31 (s, 1H), 6.93 (br s, 1H), 3.00 (s, 3H), 2.96 (s, 3H), 2.69-2.59 (m, 2H), 2.34-2.24 (m, 2H), 1.67-1.52 (m, 4H), 1.42-1.29 (m, 4H). ^{13}C NMR - (126 MHz, CDCl_3) δ 173.2 (C), 153.7 (C), 132.6 (CH), 132.0 (C), 130.5 (CH), 120.8 (C), 118.2 (C), 104.1 (C), 37.3 (CH_3), 35.5 (CH_3), 33.1 (CH_2), 29.9 (CH_2), 28.83 (CH_2), 28.80 (CH_2), 28.75 (CH_2), 24.6 (CH_2). LRMS, (ESI^+) [M+H] $^+$ 309.1 m/z .

3-Chloro-4-hydroxy-2,5-dimethyl-benzonitrile (**39**)

^1H NMR - (500MHz, CDCl_3) δ 7.29 (s, 1H), 6.21 (br s, 1H), 2.53 (s, 3H), 2.25 (s, 3H). ^{13}C NMR - (126 MHz, CDCl_3) δ 153.4 (C), 138.3 (C), 132.8 (CH), 124.2 (C), 120.8 (C), 118.0 (C), 104.9 (C), 18.7 (CH_3), 15.9 (CH_3). LRMS, (ESI^-) [M-H] $^-$ 179.9 m/z .

3-Chloro-5-ethyl-4-hydroxy-2-methyl-benzonitrile (**40**)

^1H NMR - (500MHz, CDCl_3) δ 7.32 (s, 1H), 6.14 (s, 1H), 2.66 (q, J = 7.6 Hz, 2H), 2.54 (s, 3H), 1.21 (t, J = 7.6 Hz, 3H). ^{13}C NMR - (126 MHz, CDCl_3) δ 153.0 (C), 138.3 (C), 131.4 (CH), 130.1 (C), 121.0 (C), 118.1 (C), 105.2 (C), 23.1 (CH_2), 18.8 (CH_3), 13.4 (CH_3). LRMS, (ESI^-) [M-H] $^-$ 194.0 m/z .

3-Chloro-4-hydroxy-2-methyl-5-propyl-benzonitrile (**41**)

^1H NMR - (500MHz, CDCl_3) δ 7.29 (s, 1H), 6.21 (br s, 1H), 2.60 (t, J = 7.7 Hz, 2H), 2.53 (s, 3H), 1.62-1.56 (m, 2H), 0.94 (t, J = 7.3 Hz, 3H). ^{13}C NMR - (126 MHz, CDCl_3) δ 153.2 (C), 138.3 (C), 132.2 (CH), 128.7 (C), 121.1 (C), 118.1 (C), 105.0 (C), 31.9 (CH_2), 22.2 (CH_2), 18.8 (CH_3), 13.7 (CH_3). LRMS (ESI^-) [M-H] $^-$ 207.9 m/z .

5-Butyl-3-chloro-4-hydroxy-2-methyl-benzonitrile (**42**)

^1H NMR - (500MHz, CDCl_3) δ 7.29 (s, 1H), 6.22 (br s, 1H), 2.61 (t, J = 7.8 Hz, 2H), 2.53 (s, 3H), 1.60-1.50 (m, 2H), 1.40-1.29 (m, 2H), 0.92 (t, J = 7.3 Hz, 3H). ^{13}C NMR - (126 MHz, CDCl_3) δ 153.2 (C), 138.2 (C), 132.1 (CH), 128.9 (C), 121.1 (C), 118.1 (C), 105.0 (C), 31.2 (CH_2), 29.6 (CH_2), 22.3 (CH_2), 18.7 (CH_3), 13.8 (CH_3). LRMS (ESI^-) [M-H] $^-$ 221.9 m/z .

3-Chloro-4-hydroxy-2-methyl-5-pentyl-benzonitrile (**43**)

^1H NMR - (500MHz, CDCl_3) δ 7.30 (s, 1H), 6.10 (br s, 1H), 2.62 (t, J = 7.8 Hz, 2H), 2.54 (s, 3H), 1.65-1.52 (m, 2H), 1.37-1.27 (m, 4H), 0.89 (t, J = 6.8 Hz, 3H). ^{13}C NMR - (126 MHz, CDCl_3) δ 153.1 (C), 138.2 (C), 132.2 (CH), 128.9 (C), 121.0 (C), 118.1 (C), 105.1 (C), 31.4 (CH_2), 29.9 (CH_2), 28.8 (CH_2), 22.4 (CH_2), 18.8 (CH_3), 14.0 (CH_3). LRMS, (ESI^-) [M-H] $^-$ 235.9 m/z .

3-Chloro-5-hexyl-4-hydroxy-2-methyl-benzonitrile (**44**)

¹H NMR - (500MHz, CDCl₃) δ 7.29 (s, 1H), 6.18 (br s, 1H), 2.61 (t, J = 7.8 Hz, 2H), 2.53 (s, 3H), 1.61-1.50 (m, 2H), 1.38-1.23 (m, 6H), 0.92-0.84 (m, 3H). ¹³C NMR - (126 MHz, CDCl₃) δ 153.1 (C), 138.2 (C), 132.2 (CH), 128.9 (C), 121.0 (C), 118.1 (C), 105.0 (C), 31.6 (CH₂), 30.0 (CH₂), 29.0 (CH₂), 28.9 (CH₂), 22.6 (CH₂), 18.8 (CH₃), 14.1 (CH₃). LRMS, (ESI⁻) [M-H]⁻ 249.9 m/z.

3-Chloro-5-heptyl-4-hydroxy-2-methyl-benzonitrile (**45**)

¹H NMR - (500MHz, CDCl₃) δ 7.30 (s, 1H), 6.11 (br s, 1H), 2.61 (t, J = 7.5, 2H), 2.54 (s, 3H), 1.61-1.53 (m, 2H), 1.35-1.22 (m, 8H), 0.88 (t, J = 6.2 Hz, 3H). ¹³C NMR - (126 MHz, CDCl₃) δ 153.1 (C), 138.2 (C), 132.2 (CH), 128.9 (C), 121.0 (C), 118.1 (C), 105.1 (C), 31.7 (CH₂), 30.0 (CH₂), 29.2 (CH₂), 29.09 (CH₂), 29.06 (CH₂), 22.6 (CH₂), 18.8 (CH₃), 14.1 (CH₃). LRMS, (ESI⁻), [M-H]⁻ 264.0 m/z.

5-Chloro-4-hydrox-5-octylbenzonitrile (**46**)

m.p. 60.1 – 61.8 °C. IR (neat, ν_{max}) cm⁻¹ 3362, 2927, 2849, 2230 (CN), 1595, 1471, 1316, 1241, 1168. ¹H NMR (500 MHz, CDCl₃) δ 7.49 (s, 1H), 7.34 (s, 1H), 6.07 (s, 1H), 2.66 (m, 2H), 1.59 (m, 2H), 1.49-1.17 (m, 10H), 0.88 (m, 3H). ¹³C NMR (126 MHz, CDCl₃) δ 153.4 (C), 132.9 (C), 132.2 (CH), 130.4 (CH), 120.5 (C), 118.2 (CH), 104.6 (C), 32.0 (CH₂), 30.3 (CH₂), 29.5 (CH₂), 29.5 (CH₂), 29.4 (CH₂), 29.2 (CH₂), 22.8 (CH₂), 14.3 (CH₃). HRMS (ESI⁻) m/z [M-H]⁻ calcd for C₁₅H₁₉ClNO 264.1161, found 264.1151.

General protocol for HATU amide coupling.

Triethylamine (0.07 mL, 0.49 mmol) was added to a solution of carboxylic acid (0.2 mmol), HATU (0.08 g, 0.22 mmol), and amine (0.3 mmol) in acetonitrile (0.5 mL). The reaction was stirred at RT for 16 h. The reaction mixture was partitioned between ethyl acetate (5 mL) and water (5 mL). The organic layer was separated, washed with brine, dried over MgSO₄, filtered and concentrated under reduced pressure. The residue was purified by flash silica chromatography eluting with petroleum ether to ethyl acetate in petroleum ether, then further purified by reverse phase chromatography eluting with water to MeOH if necessary to provide the amides described (29-67%).

4-(3-Chloro-5-cyano-2-hydroxy-phenyl)-N-propyl-butanamide (**19 b**)

¹H NMR - (500MHz, CDCl₃) δ 10.73 (br s, 1H), 7.95 (br t, 1H), 7.73 (s, 1H), 7.45 (s, 1H), 2.97 (m, 2H), 2.56 (t, J = 7.4 Hz, 2H), 2.04 (t, J = 7.4 Hz, 2H), 1.71 (m, 2H), 1.37 (m, 2H), 0.81 (t, J = 7.4 Hz, 3H). ¹³C NMR - (126 MHz, CDCl₃) δ 172.0 (C), 155.4 (C), 132.8 (CH), 131.9 (C), 131.4 (CH), 121.2 (C), 118.3 (C), 102.12 (C), 40.3 (CH₂), 34.3 (CH₂), 29.1 (CH₂), 25.0 (CH₂), 22.3 (CH₂), 11.4 (CH₃). LRMS, (ESI⁻) [M-H]⁻ 281.0 m/z.

5-(3-Chloro-5-cyano-2-hydroxy-phenyl)-N-ethyl-pentanamide (**20 b**)

IR (neat, ν_{max}) cm⁻¹ 3353, 2945, 2231 (CN), 1649, 1560, 1462, 1174. ¹H NMR - (500MHz, D₆-DMSO) δ 10.16 (br 1H), 7.76-7.72 (br m, 2H), 7.49 (s, 1H), 3.02 (m, 2H), 2.58 (t, J = 6.3 Hz, 2H), 2.02 (t, J = 6.3 Hz, 2H), 1.45 (m, 4H), 0.96 (t, J = 7.2 Hz, 3H). ¹³C NMR - (126 MHz, D₆-DMSO) δ 172.1 (C), 156.0 (C), 133.0 (C), 132.9 (C), 131.7 (C), 121.6 (C), 118.9 (C), 102.1 (C), 35.7 (CH₂), 33.6 (CH₂), 29.9 (CH₂), 28.9 (CH₂), 25.4

(CH₂), 15.2 (CH₃). HRMS (ESI⁺) m/z [M+Na]⁺ calcd for C₁₄H₁₇ClN₂NaO₂ 303.0871, found 303.0865.

Ethyl(2*E*)-3-5-cyano-2-hydroxy-4-methylphenylprop-2-enoate (**24**)

Potassium carbonate (0.98 g, 7.07 mmol) was added to a solution of 5-bromo-4-hydroxy-2-methyl-benzonitrile (0.50 g, 2.36 mmol) and ethyl acrylate (0.77 mL, 7.07 mL) in 1-methyl-2-pyrrolidinone (10 mL). [1,3-bis(2,4,6-trimethylphenyl)-2,3-dihydro-1*H*-imidazol-2-ylidene]({2-[(di-methylamino)methyl]phenyl})palladiumium chloride (SingaCycle®) was added to the suspension and the reaction was sealed under nitrogen and heated at 100°C for 48 h. The reaction mixture was cooled to RT and diluted with ethyl acetate (50 mL) and filtered through a celite pad. The filtrate was washed with 1M HCl (aq) (25 mL), 0.5 M LiCl (aq) (25 mL), brine (25 mL), dried over MgSO₄ filtered and concentrated under vacuum. The residue was purified by flash silica chromatography eluting with petroleum ether to 15% ethyl acetate in petroleum ether to provide the title compound as a white solid (0.16 g, 29%). m.p. 142.6-149.8 °C. IR (neat, ν_{max}) cm⁻¹ 2923, 2221, 1600, 1274. ¹H NMR (500 MHz, D₆-DMSO) δ 11.30 (br s, 1H) 8.07 (s, 1H), 7.73 (d, J = 16 Hz, 1H), 6.90 (s, 1H), 6.70 (d, J = 16 Hz, 1H), 4.17 (d, J = 7.2 Hz, 2H), 2.38 (s, 3H), 1.24 (t, J = 7.2 Hz, 3H). ¹³C NMR (126 MHz, D₆-DMSO) δ 160.9 (C), 160.6 (C), 145.4 (C), 138.2 (CH), 134.4 (CH), 120.3 (C), 119.4 (CH), 118.5 (C), 118.1 (CH), 103.19 (CN), 60.4 (CH₂), 20.5 (CH₃), 14.6 (CH₃). HRMS (ESI⁻) m/z [M-H]⁻ calcd for C₁₃H₁₂NO₃ 230.0823, found 230.0814.

Ethyl 3-(5-cyano-2-hydroxy-4-methyl-phenyl)propanoate (**25**)

Triethylsilane (0.50 g, 4.32 mmol) was added to a solution ethyl (*E*)-3-(5-cyano-2-hydroxy-4-methyl-phenyl)prop-2-enoate (0.10 g, 0.43 mmol) and 10% palladium on carbon (4 mg, 0.04 mmol) in ethanol (5 mL). The reaction mixture was stirred at RT for 16 h. Further triethylsilane (0.50 g, 4.32 mmol) was added and the reaction mixture was stirred for a further 16 h. The nitrogen purged reaction mixture was filtered through a pad of celite, the filtrate was partitioned between 1M HCl (aq) (10 mL) and ethyl acetate (2 x 20 mL). The combined organics were separated, dried over MgSO₄, filtered and concentrated under vacuum. The residue was purified by flash silica chromatography, eluting with petroleum ether to 50% ethyl acetate in petroleum ether to provide the title compound as a white solid (0.08 g, 77%). IR (neat, ν_{max}) cm⁻¹ 3496, 2927, 2225 (CN), 1716, 1199, 1250. ¹H NMR (500 MHz, CDCl₃) δ 8.25 (s, 1H), 7.32 (s, 1H), 6.80 (s, 1H), 4.16 (q, J = 7.3 Hz, 2H), 2.84 (m, 2H), 2.70 (m, 2H), 2.44 (s, 3H), 1.25 (t, J = 7.3 Hz). ¹³C NMR (126 MHz, CDCl₃) δ 175.9 (C), 158.4 (C), 142.5 (C), 135.1 (CH), 125.8 (C), 119.0 (CH), 118.6 (C), 104.3 (C), 61.8 (CH₂), 35.0 (CH₂), 24.0 (CH₂), 20.1 (CH₃), 14.0 (CH₃). HRMS (ESI⁺) m/z [M+H]⁺ calcd for C₁₃H₁₅NNaO₃ 256.0944, found 256.0941.

Ethyl 3-(3-chloro-5-cyano-2-hydroxy-4-methyl-phenyl)propanoate (**26**)

Sulfuryl chloride (0.02 mL, 0.26 mmol) was added to a solution ethyl 3-(5-cyano-2-hydroxy-4-methyl-phenyl)propanoate (0.05 g, 0.21 mmol) in diethyl ether (1 mL). The reaction mixture was stirred at RT for 96 h. Further sulfuryl

chloride (0.02 mL, 0.26 mmol) was added and the reaction mixture was stirred for a further 16 hours. The reaction mixture was partitioned between 1M HCl (aq) (10 mL) and ethyl acetate (2 x 20 mL). The combined organics were separated, dried over MgSO₄, filtered and concentrated under vacuum. The residue was purified by flash silica chromatography, eluting with petroleum ether to 25% ethyl acetate in petroleum ether to provide the title compound as a white solid (0.043 g, 75%). IR (neat, ν_{\max}), cm⁻¹ 3340, 2997, 2228 (CN), 1712, 1210, 1177. ¹H NMR (500 MHz, CDCl₃) δ 7.33 (s, 1H), 7.03 (s, 1H), 4.14 (q, J = 7.1 Hz, 2H), 2.94 (t, J = 7.1 Hz, 2H), 2.65 (t, J = 7.1 Hz, 2H), 2.55 (s, 3H), 1.24 (t, J = 7.1 Hz, 3H). ¹³C NMR (126 MHz, CDCl₃) δ 173.6 (C), 153.6 (C), 139.4 (C), 132.6 (CH), 126.7 (C), 117.9 (C), 105.3 (C), 61.1 (CH₂), 33.7 (CH₂), 25.3 (CH₂), 18.9 (CH₃), 14.2 (CH₃). HRMS (ESI⁻) m/z [M-H]⁻ calcd for C₁₃H₁₃NO₃ 266.0589, found 266.0576.

General protocol for 1,5,7-triazabicyclo[4.4.0]dec-5-ene amide formation.

Amine (0.33 mmol) was added to a solution of 1,5,7-triazabicyclo[4.4.0]dec-5-ene (0.04 g, 0.26 mmol) and ester (0.13 mmol) in acetonitrile (0.5 mL). The reaction was stirred at RT for 5-40 h. The reaction mixture was partitioned between ethyl acetate (25 mL) and water (25 mL). The organic layer was separated, washed with brine, dried over MgSO₄, filtered and concentrated under reduced pressure. The residue was purified by flash silica chromatography eluting with petroleum ether to 30-50% ethyl acetate in petroleum ether to provide the amides described (27-80%).

6-(3-Chloro-5-cyano-2-methoxy-phenyl)-N-methyl-hexanamide (21 a)

IR (neat, ν_{\max}), cm⁻¹ 3300, 2938, 2230 (CN), 1639, 1557, 1281. ¹H NMR - (500MHz, CDCl₃) δ 7.52 (d, J = 2.0 Hz, 1H), 7.37 (d, J = 2.0 Hz, 1H), 5.44 (br s, 1H), 3.88 (s, 3H), 2.80 (d, J = 5.0 Hz, 3H), 2.65 (t, J = 7.6 Hz, 2H), 2.17 (t, J = 7.6 Hz, 2H), 1.68 (m, 2H), 1.59 (m, 2H), 1.37 (m, 2H). ¹³C NMR - (126 MHz, CDCl₃) δ 173.5 (C), 158.4 (C), 139.4 (C), 132.6 (CH), 132.0 (CH), 129.1 (C), 117.8 (C), 108.6 (C), 61.3 (CH₃), 36.6 (CH₂), 30.1 (CH₂), 30.0 (CH₂), 29.1 (CH₂), 26.4 (CH₂), 25.5 (CH₃). HRMS (ESI⁺) m/z [M+Na]⁺ calcd for C₁₅H₁₉ClN₂NaO₂ 317.1027, found 317.1019.

7-(3-Chloro-5-cyano-2-methoxy-phenyl)-N-methyl-heptanamide (22 a)

¹H NMR - (500MHz, CDCl₃) δ 7.52 (d, J = 2.0 Hz, 1H), 7.37 (d, J = 2.0 Hz, 1H), 5.41 (br s, 1H), 3.88 (s, 3H), 2.80 (d, J = 5.0 Hz, 3H), 2.64 (t, J = 7.9 Hz, 2H), 2.16 (t, J = 7.6 Hz, 2H), 1.69-1.52 (m, 4H), 1.42-1.28 (m, 4H). ¹³C NMR - (126 MHz, CDCl₃) δ 173.5 (C), 158.2 (C), 139.4 (C), 132.4 (C), 131.8 (C), 128.9 (C), 117.7 (C), 108.4 (C), 61.1 (CH₃), 36.6 (CH₂), 30.0 (CH₂), 29.9 (CH₂), 29.1 (CH₂), 29.0 (CH₂), 26.3 (CH₃), 25.5 (CH₂). LRMS, (ESI⁺) [M+H]⁺ 309.1 m/z.

7-(3-Chloro-5-cyano-2-methoxy-phenyl)-N,N-dimethyl-heptanamide (23 a)

¹H NMR - (500MHz, CDCl₃) δ 7.52 (s, 1), 7.37 (s, 1H), 3.88 (s, 3H), 2.99 (s, 3H), 2.94 (s, 3H), 2.64 (m, 2H), 2.30 (m, 2H), 1.70-1.53 (m, 4H), 1.43-1.32 (m, 4H). ¹³C NMR - (126 MHz,

CDCl₃) δ 173.0 (C), 158.2 (C), 139.5 (C), 132.4 (C), 131.8 (C), 128.9 (C), 117.7 (C), 108.4 (C), 61.1 (CH₃), 37.3 (CH₃), 35.4 (CH₃), 33.2 (CH₂), 30.1 (CH₂), 29.9 (CH₂), 29.2 (CH₂), 29.2 (CH₂), 25.0 (CH₂). LRMS, (ESI⁺) [M+H]⁺ 323.1 m/z.

N-Butyl-3-(3-chloro-5-cyano-2-hydroxy-4-methyl-phenyl)propenamide (27)

IR (neat, ν_{\max}), cm⁻¹ 3369, 2928, 2220 (CN), 1632, 1562, 1157. ¹H NMR (500MHz, CDCl₃) δ 10.35 (br s, 1H), 7.24 (s, 1H), 5.55 (br s, 1H), 3.26 (m, 2H), 2.91 (m, 2H), 2.59 (m, 2H), 2.54 (s, 3H), 1.45 (m, 2H), 1.28 (m, 2H), 0.90 (t, J = 7.5 Hz, 3H). ¹³C NMR - (126 MHz, CDCl₃) δ 173.6 (C), 155.6 (C), 140.0 (C), 132.6 (CH), 127.4 (C), 123.9 (C), 118.3 (C), 104.0 (C), 39.9 (CH₂), 36.3 (CH₂), 31.4 (CH₂), 25.0 (CH₂), 19.9 (CH₂), 18.9 (CH₃), 13.6 (CH₃). HRMS (ESI⁺) m/z [M+Na]⁺ calcd for C₁₅H₁₉ClN₂NaO₂ 317.1027, found 317.1019.

AUTHOR INFORMATION

Corresponding Author

* Simon E. Ward, Sêr Cymru Professor in Translational Drug Discovery & Director of Medicines Discovery Institute, Cardiff University, Park Place, Cardiff, CF10 3AT, UK

Author Contributions

All authors have given approval to the final version of the manuscript.

Funding Sources

This work was supported by the Biotechnology and Biological Sciences Research Council [Grant Ref: BB/L017180/1] iCASE with Novartis Institute for Tropical Diseases.

Acknowledgment

We would like to acknowledge and thank Rima Palkar and Nahdiah Ghafar for carrying out the *T. b. brucei* growth inhibition assays.

ABBREVIATIONS

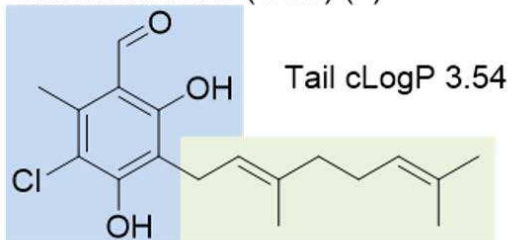
AAT, African animal trypanosomiasis; AF, ascofuranone; CCB, collettichlorin B; CNS, central nervous system; HAT, human African trypanosomiasis; LipE, lipophilic efficiency; MPO, multi-parameter-optimisation; NECT, Nifurtimox and Eflornithine combination therapy; TAO, trypanosome alternative oxidase; *T. b. b.*, *trypanosoma brucei brucei*; TBD, 1,5,7-triazabicyclo[4.4.0]dec-5-ene

REFERENCES

- (1) World Health Organisation. *Control and surveillance of human African trypanosomiasis*; Geneva, 2013.
- (2) T. Jacobs, R.; Nare, B.; A. Phillips, M. State of the Art in African Trypanosome Drug Discovery. *Curr. Top. Med. Chem.* **2011**, *11* (10), 1255-1274 DOI: 10.2174/156802611795429167.
- (3) Stich, A.; Ponte-Sucre, A.; Holzgrabe, U. Do we need new drugs against human African trypanosomiasis? *Lancet Infect. Dis.* **2013**, *13* (9), 733-734 DOI: 10.1016/S1473-3099(13)70191-9.
- (4) Delespau, V.; Dekoning, H. Drugs and drug resistance in African trypanosomiasis. *Drug Resist. Updat.* **2007**, *10* (1-2), 30-50 DOI: 10.1016/j.drug.2007.02.004.
- (5) Baker, N.; de Koning, H. P.; Mäser, P.; Horn, D. Drug resistance in African trypanosomiasis: the melarsoprol and

- pentamidine story. *Trends Parasitol.* **2013**, 29 (3), 110–118 DOI: 10.1016/j.pt.2012.12.005.
- (6) Bruce, D. Preliminary report on the tsetse fly disease or nagana in Zululand. *Bennet & Davis. Durban* **1895**, 28.
- (7) Nagle, A. S.; Khare, S.; Kumar, A. B.; Supek, F.; Buchynskyy, A.; Mathison, C. J. N.; Chennamaneni, N. K.; Pendem, N.; Buckner, F. S.; Gelb, M. H.; et al. Recent Developments in Drug Discovery for Leishmaniasis and Human African Trypanosomiasis. *Chem. Rev.* **2014** DOI: 10.1021/cr500365f.
- (8) Matthews, K. R. The developmental cell biology of *Trypanosoma brucei*. *Journal of cell science*. January 2005, pp 283–290.
- (9) Wang, C. C. Molecular Mechanisms and Therapeutic Approaches to the Treatment of African Trypanosomiasis. *Annu. Rev. Pharmacol. Toxicol.* **1995**, 35 (1), 93–127 DOI: 10.1146/annurev.pa.35.040195.000521.
- (10) David Barry, J.; McCulloch, R. Antigenic variation in trypanosomes: Enhanced phenotypic variation in a eukaryotic parasite. In *Advances in Parasitology Volume 49*; Advances in Parasitology; Elsevier, 2001; Vol. 49, pp 1–70.
- (11) Fevre, E. M.; Wissmann, B. V.; Welburn, S. C.; Lutumba, P. The Burden of Human African Trypanosomiasis. *PLoS Negl. Trop. Dis.* **2008**, 2 (12), e333 DOI: 10.1371/journal.pntd.0000333.
- (12) Wilson, S. G.; Morris, K. R. S.; Lewis, I. J.; Krog, E. The effects of trypanosomiasis on rural economy*. *Bull. World Health Organ.* **1963**.
- (13) Fairlamb, A. H. Chemotherapy of human African trypanosomiasis: Current and future prospects. *Trends in Parasitology*. 2003, pp 488–494.
- (14) Pépin, J.; Milord, F. The treatment of human African trypanosomiasis. *Adv. Parasitol.* **1994**, 33, 1–47 DOI: 10.1016/S0065-308X(08)60410-8.
- (15) Kennedy, P. G. Clinical features, diagnosis, and treatment of human African trypanosomiasis (sleeping sickness). *Lancet Neurol.* **2013**, 12 (2), 186–194 DOI: 10.1016/S1474-4422(12)70296-X.
- (16) Burri, C.; Brun, R. Eflornithine for the treatment of human African trypanosomiasis. *Parasitol. Res.* **2003**, 90 Suppl 1, S49–52 DOI: 10.1007/s00436-002-0766-5.
- (17) Menzies, S. K.; Tulloch, L. B.; Florence, G. J.; Smith, T. K. The trypanosome alternative oxidase: a potential drug target? *Parasitology* **2016**, First View, 1–9 DOI: 10.1017/S003182016002109.
- (18) Nihei, C.; Fukai, Y.; Kita, K. Trypanosome alternative oxidase as a target of chemotherapy. *Biochim. Biophys. Acta* **2002**, 1587 (2–3), 234–239.
- (19) Chaudhuri, M.; Ajayi, W.; Hill, G. C. Biochemical and molecular properties of the *Trypanosoma brucei* alternative oxidase. *Mol. Biochem. Parasitol.* **1998**, 95 (1), 53–68.
- (20) Jeacock, L.; Baker, N.; Wiedemar, N.; Mäser, P.; Horn, D. Aquaglyceroporin-null trypanosomes display glycerol transport defects and respiratory-inhibitor sensitivity. *PLoS Pathog.* **2017**, 13 (3), 1–16 DOI: 10.1371/journal.ppat.1006307.
- (21) Kido, Y.; Shiba, T.; Inaoka, D. K.; Sakamoto, K.; Nara, T.; Aoki, T.; Honma, T.; Tanaka, A.; Inoue, M.; Matsuoka, S.; et al. Crystallization and preliminary crystallographic analysis of cyanide-insensitive alternative oxidase from *Trypanosoma brucei brucei*. *Acta Crystallogr. Sect. F. Struct. Biol. Cryst. Commun.* **2010**, 66 (Pt 3), 275–278 DOI: 10.1107/S1744309109054062.
- (22) Saimoto, H.; Kido, Y.; Haga, Y.; Sakamoto, K.; Kita, K. Pharmacophore identification of ascofuranone, potent inhibitor of cyanide-insensitive alternative oxidase of *Trypanosoma brucei*. *J. Biochem.* **2013**, 153 (3), 267–273 DOI: 10.1093/jb/mvs135.
- (23) West, R. A.; Doherty, O. G. O.; Askwith, T.; Atack, J.; Beswick, P.; Laverick, J.; Pennicott, L. E.; Williams, G.; Ward, S. E. African trypanosomiasis: Synthesis & SAR enabling novel drug discovery of ubiquinol mimics for trypanosome alternative oxidase. *Eur. J. Med. Chem.* **2017**, In Press DOI: 10.1016/j.ejmech.2017.09.067.
- (24) Yabu, Y.; Suzuki, T.; Nihei, C. I.; Minagawa, N.; Hosokawa, T.; Nagai, K.; Kita, K.; Ohta, N. Chemotherapeutic efficacy of ascofuranone in *Trypanosoma vivax*-infected mice without glycerol. *Parasitol. Int.* **2006**, 55 (1), 39–43 DOI: 10.1016/j.parint.2005.09.003.
- (25) Pardridge, W. M. The blood-brain barrier: Bottleneck in brain drug development. *NeuroRX* **2005**, 2 (1), 3–14 DOI: 10.1602/neurorx.2.1.3.
- (26) Wager, T. T.; Hou, X.; Verhoest, P. R.; Villalobos, A. Moving beyond Rules: The Development of a Central Nervous System Multiparameter Optimization (CNSMPO) Approach To Enable Alignment of Druglike Properties. *ACS Chem. Neurosci.* **2010**, 1 (6), 435–449 DOI: 10.1021/cn100008c.
- (27) Casey, M. L.; Kemp, D. S.; Paul, K. G.; Cox, D. D. Physical organic chemistry of benzisoxazoles. I. Mechanism of the base-catalyzed decomposition of benzisoxazoles. *J. Org. Chem.* **1973**, 38 (13), 2294–2301 DOI: 10.1021/jo00953a006.
- (28) Kajigaeshi, S.; Kakinami, T.; Okamoto, T.; Nakamura, H.; Fujikawa, M. Halogenation Using Quaternary Ammonium Polyhalides. IV. Selective Bromination of Phenols by Use of Tetraalkylammonium Tribromides. *Bull. Chem. Soc. Jpn.* **1987**, 60 (11), 4187–4189 DOI: 10.1246/bcsj.60.4187.
- (29) Li, H.; Zhong, Y.-L.; Chen, C.; Ferraro, A. E.; Wang, D. A Concise and Atom-Economical Suzuki-Miyaura Coupling Reaction Using Unactivated Trialkyl- and Triarylboranes with Aryl Halides. *Org. Lett.* **2015**, 17 (14), 3616–3619 DOI: 10.1021/acs.orglett.5b01720.
- (30) Enache, L. A.; Kennedy, I.; Sullins, D. W.; Chen, W.; Ristic, D.; Stahl, G. L.; Dzekhtser, S.; Erickson, R. A.; Yan, C.; Muellner, F. W.; et al. Development of a Scalable Synthetic Process for DG-051B, A First-in-Class Inhibitor of LTA4H. *Org. Process Res. Dev.* **2009**, 13 (6), 1177–1184 DOI: 10.1021/op90023j.
- (31) Sabot, C.; Kumar, K. A.; Meunier, S.; Mioskowski, C. A convenient aminolysis of esters catalyzed by 1,5,7-triazabicyclo[4.4.0]dec-5-ene (TBD) under solvent-free conditions. *Tetrahedron Lett.* **2007**, 48 (22), 3863–3866 DOI: 10.1016/j.tetlet.2007.03.146.
- (32) Ryckmans, T.; Edwards, M. P.; Horne, V. A.; Correia, A. M.; Owen, D. R.; Thompson, L. R.; Tran, I.; Tutt, M. F.; Young, T. Rapid assessment of a novel series of selective CB2 agonists using parallel synthesis protocols: A Lipophilic Efficiency (LipE) analysis. *Bioorganic Med. Chem. Lett.* **2009**, 19 (15), 4406–4409 DOI: 10.1016/j.bmcl.2009.05.062.
- (33) Kondreddi, R. R.; Jiricek, J.; Rao, S. P. S.; Lakshminarayana, S. B.; Camacho, L. R.; Rao, R.; Herve, M.; Bifani, P.; Ma, N. L.; Kuhen, K.; et al. Design, Synthesis, and Biological Evaluation of Indole-2-carboxamides: A Promising Class of Antituberculosis Agents. *J. Med. Chem.* **2013**, 56 (21), 8849–8859 DOI: 10.1021/jm4012774.
- (34) Ng, P. S.; Manjunatha, U. H.; Rao, S. P. S.; Camacho, L. R.; Ma, N. L.; Herve, M.; Noble, C. G.; Goh, A.; Peukert, S.; Diagona, T. T.; et al. Structure activity relationships of 4-hydroxy-2-pyridones: A novel class of antituberculosis agents. *Eur. J. Med. Chem.* **2015**, 106, 144–156 DOI: 10.1016/j.ejmech.2015.10.008.

Colletochlorin B (CCB) (2)



Aromatic
cLogP 2.68



Decrease
cLogP



TAO pIC50

